Nematic antiferromagnetism and deconfined criticality from the interplay between electron-phonon and electron-electron interactions

Chao Wang, Yoni Schattner, and Steven A. Kivelson

Phys. Rev. B **104**, L081110 — Published 18 August 2021

DOI: 10.1103/PhysRevB.104.L081110

Nematic Antiferromagnetism and Deconfined Criticality from the Interplay between Electron-Phonon and Electron-Electron Interactions

Chao Wang[1], Yoni Schattner[1,2], Steven A. Kivelson[1]
1) Department of Physics, Stanford University, Stanford, CA 94305 and
2) Stanford Institute for Materials and Energy Sciences,
SLAC National Accelerator Laboratory and Stanford University, Menlo Park, CA 94025

Systems with strong electron-phonon couplings typically exhibit various forms of charge order, while strong electron-electron interactions lead to magnetism. We use determinant quantum Monte Carlo (DQMC) calculations to solve a model on a square lattice with a caricature of these interactions. In the limit where electron-electron interactions dominate it has antiferromagnetic (AF) order, while where electron-phonon coupling dominates there is columnar valence-bond solid (VBS) order. We find a novel intervening phase that hosts coexisting nematic and antiferromagnetic orders. We have also found evidence of a Landau-forbidden continuous quantum phase transition with an emergent $O(4)$ symmetry between the VBS and the nematic antiferromagnetic phases.

Introduction: The interplay of electron-electron and electron-phonon interactions is crucial in determining the nature of the ground state in electronic systems. While electron-electron interactions conventionally give rise to magnetism, a large electron-phonon coupling can give rise to, among other things, superconductivity, charge or bond density wave orders, as well as nematic order. It is also possible that the interplay between the two sorts of interactions can stabilize novel intermediate quantum phases, including spin-liquids, or exotic "deconfined quantum critical" transitions between otherwise conventional broken-symmetry phases.

In this work we consider fermions on the two dimensional square lattice with repulsive electron-electron interactions, as well as a coupling to local pseudo-spin degrees of freedom that are a caricature of optical phonons. We compute thermodynamic correlation functions using determinant quantum Monte Carlo (DQMC) [1, 2] and restrict our attention to the case in which the average electron density is $n = 1$ electron per site, so the simulations are free of the famous fermion minus sign problem.

Our model is conceived to exhibit two previously studied phases in extremal limits, an antiferromagnetic (AF) and a columnar valence-bond-solid (VBS) phase [3, 4] (shown in cartoons in Fig. 1) both of which are incompressible at temperature $T \to 0$, and hence insulating. In addition to these two phases we find a novel insulating nematic antiferromagnetic (NAF) phase, in which the lattice C_4 rotation symmetry is broken down to C_2 (as it is in the VBS phase) but the only translation symmetry breaking is associated with the AF order.

There are a number of phase transitions of interest in this phase diagram. Most notably, along a portion of the phase boundary between the VBS and NAF phases (dashed line in the figure), the transition is continuous and exhibits an emergent $O(4)$ symmetry that unifies the AF and VBS order parameters. This is an example of a deconfined quantum critical point (DQCP) [5] at which larger symmetries are predicted to emerge. Beyond a tricritical point, this transition becomes first order (as indicated by the solid line). Our results are in line with previous numerical studies [6–26] of various DQCPs. In particular, the emergent $O(4)$ symmetry in our study is similar to that found in studies [16, 27] of the DQCP between an AF and a Kekulé phase or between an AF and a nematic paramagnetic phase. Interestingly, in these cases the transition cannot be described in terms of the proliferation of topological point defects in either the Z_2 or the O(3) orders. In constrast, such a description is possible for the closely related case of a DQCP between phases with a $U(1)$ and a Z_4 order, for which there is good theoretical [5, 28] and numerical evidence [15, 22]

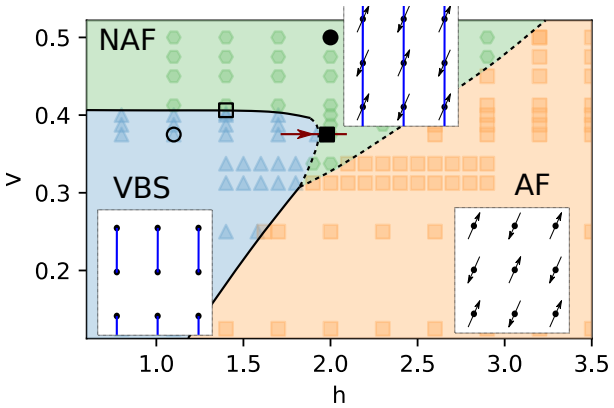

FIG. 1. Phase diagram in the $h - V$ plane with $\alpha = 0.7, \tilde{V} = 0.5$. Data points in the VBS, NAF and AF phases are shown in blue, green, and orange, respectively. The density of the symbols reflects the frequency of the numerical experiments and carries no physical meaning. The lines are a guides to the eye. Solid (dashed) lines indicate first (second) order transitions. The insets illustrate the ground state deep in the ordered phases. Blue lines represent strong bonds, and the arrows represent the spin orientations. The data presented in Figs. 2, 4(a) 4(b), and 5 correspond to the black filled circle, filled square, empty square and empty circle, respectively. Fig. 3 examines the phase transition indicated by the dark red arrow.

of an emergent $O(4)$ symmetry.

More generally, these considerations are reminiscent of earlier theories of a DQCP between VBS and AF phases, where duality arguments [5, 28] suggested an $O(5)$ symmetry that unifies Néel ($O(3)$) and VBS (Z_4) order parameters. However, rigorous bounds on critical exponents obtained from conformal bootstrap calculations [29] have raised doubts about the existence of such a DQCP. Indeed, elsewhere in the phase diagram we find a direct transition from an AF to a VBS phase, but this transition appears always to be first order - we find no signs of a putative DQCP with emergent $O(5)$ symmetry.

In addition, there is a Landau-allowed continuous transition along the phase boundary between the AF and NAF phases. We find no evidence of two-phase coexistence near any of the first order transitions [30].

The Model: Our model is defined on the two dimensional square lattice, with electrons that interact with onsite repulsive Hubbard interactions. We also introduce pseudo-spin variables that are a caricature of phonons. Each pseudo-spin variable lives on a nearest-neighbor bond and can be thought of as representing the local lattice distortion.

The Hamiltonian consists of three parts

$$H = H_{\rm e} + H_{\rm ph} + H_{\rm int}. \tag{1}$$

$H_{\rm e}$ is the Hubbard model for spin-$\frac{1}{2}$ fermions at half-filling

$$\begin{aligned} H_{\rm e} = &-t \sum_{\langle i,j\rangle,\sigma} \left(c^\dagger_{i,\sigma} c_{j,\sigma} + \text{h.c.} \right) \\ &+ U \sum_i \left(n_{i,\uparrow} - \frac{1}{2} \right) \left(n_{i,\downarrow} - \frac{1}{2} \right), \end{aligned} \tag{2}$$

where i denotes sites and $\langle i,j\rangle$ denotes nearest-neighbors.

$H_{\rm ph}$ is the bare phonon piece:

$$\begin{aligned} H_{\rm ph} = &-V \sum_{\substack{i \\ k \square l}}^{j} \left(\tau^z_{ij}\tau^z_{kl} + \tau^z_{ik}\tau^z_{jl} + \tau^z_{ij}\tau^z_{kl}\tau^z_{ik}\tau^z_{jl} \right) \\ &+ (V+\tilde{V}) \sum_{\langle j,i,k\rangle} \tau^z_{ji}\tau^z_{ik} + 6\tilde{V} \sum_{\langle i,j\rangle} \tau^z_{ij} - h \sum_{\langle i,j\rangle} \tau^x_{ij}, \end{aligned} \tag{3}$$

where the pseudo-spin $\vec{\tau}_{ij} = \vec{\tau}_{ji}$ represents a two-state "phonon" mode on each nearest-neighbor bond, the sum over $\langle j,i,k\rangle$ is over pairs of bonds with a common vertex, the various terms proportional to V and $\tilde{V}$ (both assumed positive) determine the favored "classical configurations" of the pseudo-spins, and the transverse field h gives them dynamics. The classical states can be visualized in a lattice-gas representation, in which a "strong" bond on which $\tau^z_{ij} = 1$ is thought to be occupied by a dimer. The preferred (zero energy) configurations for large $\tilde{V}$ correspond to those of the hard-core dimer model [4], such that no two strong bonds share a common vertex (i.e. the dimers satisfy a hard-core constraint). Positive V on the other hand, favors plaquette configurations with exactly one pair of dimers on opposite sides. The classical ($h \to 0$) ground-states of $H_{\rm ph}$ for $\tilde{V} > V > 0$ are the 4 symmetry-related columnar VBS states of the sort shown in the lower left inset in Fig. 1 with dimers on the blue bonds, while for $V > \tilde{V} > 0$, they are the 2 nematic states of the sort shown in the upper inset.

Lastly the electrons are coupled to the pseudo-spins by

$$H_{\rm int} = -\alpha t \sum_{\langle i,j\rangle,\sigma} \tau^z_{ij} \left[c^\dagger_{i,\sigma} c_{j,\sigma} + \text{h.c.} \right]. \tag{4}$$

The interactions in our model are such that the ground-state is an AF for $h \to \infty$ and a columnar VBS phase as $h \to 0$ so long as $V \ll \tilde{V}$ and α is sufficiently big [31].

Calculational particulars: In order to use the DQMC technique without encountering the sign problem, we restrict ourselves to the case of half-filling of fermions. We apply a discrete Hubbard-Stratonovich decoupling in the spin channel to represent the Hubbard interaction [30]. We have performed DQMC simulations at finite temperatures, with imaginary time discretization $\Delta\tau = 0.1$ and systems of linear size up to $L = 18$ and down to temperatures $T = 1/18$. Throughout this letter we use periodic boundary conditions, and fix $t = 1, U = 3, \tilde{V} = 0.5$, and $\alpha = 0.7$ unless mentioned otherwise. As illustrated in Fig. 1, we then explore the zero temperature phase diagram as a function of h and V. We identify the different ordered states by the divergence of the appropriate susceptibility as the system size is increased [30].

Where C_4 symmetry is spontaneously broken, in order to avoid complications due to metastable domain structures, we typically seed our DQMC runs with a configuration obtained by introducing an explicit symmetry breaking field for an initial 3000 DQMC steps, but then removing this field so that the model has the requisite C_4 symmetry for all subsequent steps. We illustrate our most significant findings with representative figures in the main text, but present more complete data in the Supplemental Material.

Nematic antiferromagnet: Fig. 1 shows that the NAF arises as an intermediate phase [32]. In Fig. 2 we show the spin and pseudo-spin susceptibilities as functions of momentum ($\mathbf{q}$) at a representative point in this phase. The susceptibilities are defined as

$$\chi(\mathbf{q}) = \frac{1}{L^2} \sum_{i,j} \int_0^\beta d\tau \ \langle \vec{S}_i(\tau) \cdot \vec{S}_j(0) \rangle e^{i\mathbf{q}\cdot(\mathbf{r}_i - \mathbf{r}_j)} \tag{5}$$

$$D_a(\mathbf{q}) = \frac{1}{L^2} \sum_{\langle i,j\rangle_a \langle k,l\rangle_a} \int_0^\beta d\tau \ \langle \tau^z_{ij}(\tau)\tau^z_{kl}(0) \rangle e^{i\mathbf{q}\cdot(\mathbf{r}_{ij} - \mathbf{r}_{kl})}, \tag{6}$$

where $\vec{S}_i$ is the electron spin, $\mathbf{r}_{ij}$ is the position of the center of the bond $\langle i,j\rangle$, and the subscript $a = x$ or

y signifies the orientation of the bond. That this is a magnetically ordered state is shown by the presence of a Bragg peak in $\chi(\mathbf{q})$ as $T \to 0$, as is evident in the figure and which we have corroborated by finite size scaling. The fact that both correlation functions depend on the direction of $\mathbf{q}$ shows that the state spontaneously breaks C_4 symmetry down to C_2, i.e. that it is nematic.

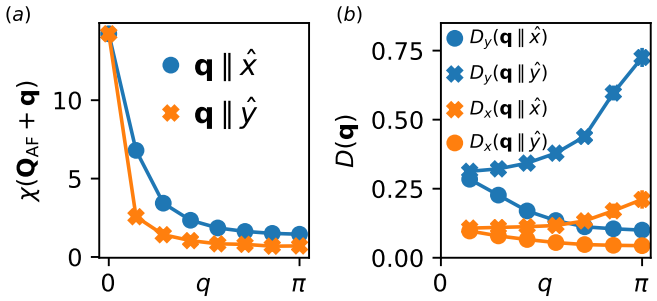

FIG. 2. Correlation functions in momentum space $\mathbf{q}$ in the NAF phase ($h = 2.0, V = 0.5$ - the black filled circle in Fig. 1 - with $L = \beta = 14$). (a) Static spin-spin susceptibility as a function of deviation from AF ordering vector $\mathbf{Q}_{\rm AF} = (\pi, \pi)$. (b) Static bond-bond susceptibility for x- and y-direction bonds.

VBS to NAF transition: As shown in Fig. 1, as a function of increasing V at fixed small h, there is a strongly first order transition (indicated by a solid line) from a VBS to the NAF, characterized by a discontinuous jump in first derivatives of free energy [30]. Indeed, since the NAF spontaneously breaks time-reversal (TR) symmetry but is invariant under the product of translation and time-reversal (TrTR) while the VBS preserves TR but breaks TrTR, conventional Landau theory implies the transition must be first order. However, at larger h, the phase boundary bends sharply and, beyond a tri-critical point, the transition becomes continuous (dashed line) within our numerical resolution. Eventually the phase boundary ends at a bi-critical point. (We have not yet explored these multicritical points in detail, but we note that since the phase boundary that links them is exotic, they may have unusual features as well.)

We now focus on the continuous VBS-NAF transitions. To be concrete, we fix $V = 0.375$ and study the finite size scaling behavior of the static AF and VBS susceptibilities $\chi_{\rm AF}, \chi_{\rm VBS}$ as a function of h. These are given by the expressions in Eqn. 5 and 6 evaluated at $\mathbf{Q}_{\rm AF} = (\pi, \pi)$ and $\mathbf{Q}_{\rm VBS} = (0, \pi)$, respectively, with the bond direction set to $a = y$. Since both the VBS and the NAF phases break the C_4 rotational symmetry, in the remaining calcuations reported here we have applied a small explicit C_4 symmetry breaking in our simulations to stabilize our results, by making the hopping matrix element t to be slightly different in the two directions (with $t_x = 0.97, t_y = 1.0$) [33]. As a consequence, the pseudo-spins correlations are stronger for y-directed bonds, which we will refer to as the nematic direction. The nematic direction also corresponds to the direction of the ordering wavevector in the VBS state. (See inset to Fig. 1.) Note that in the presence of this explicit symmetry breaking, the VBS order-has Z_2 (Ising) character, corresponding to the breaking of translational symmetry.

Assuming the transition is continuous, on theoretical grounds we expect conformal symmetry with dynamical critical exponent $z = 1$. We thus scale space and time together by taking $\beta = L$ and express the susceptibilities in the scaling forms (neglecting corrections to scaling)

$$\chi(L) = L^{d+1-\eta}\ \tilde{\chi}\left[(h - h_c)L^{1/\nu}\right], \tag{7}$$

where $d = 2$, χ is either $\chi_{\rm AF}$ or $\chi_{\rm VBS}$, and ν is the correlation length and η the anomalous exponent.

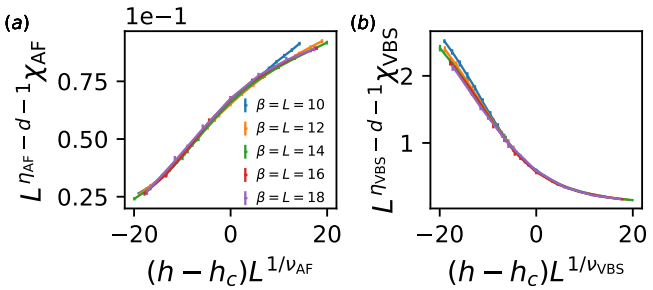

FIG. 3. Finite size scaling collapses of AF and VBS susceptibilities along the dark red arrow in Fig. 1 ($V = 0.375$). The location of the transition is identified as $h_c \approx 1.98$. The critical exponents for the two different orders are within error bars from each other.

In Fig. 3 we show the finite-size scaling collapse results for these two susceptibilities taking $h_c \approx 1.98$. We obtain $1/\nu_{\rm AF} = 2.2 \pm 0.4, 1/\nu_{\rm VBS} = 2.0 \pm 0.4$ and $\eta_{\rm AF} = 0.65 \pm 0.2, \eta_{\rm VBS} = 0.65 \pm 0.2$. These results indicate a direct and continuous transition between the two phases. The near equivalence of the exponents extracted from the AF and VBS susceptibilities hints at an emergent $O(4)$ symmetry that unifies the three components of the spin AF with the single component VBS. The Binder ratios close to the transition provides further support for the continuous nature of the transition [30].

Emergent $O(4)$ Symmetry: To further investigate the possibility of a larger emergent symmetry at the critical point, we examine the relation between one component of the AF order parameter $\vec{\phi}_{\rm AF}$ and the y-component of VBS order parameter $\phi_{\rm VBS}$, defined as:

$$\vec{\phi}_{\rm AF} \equiv \frac{1}{\mathcal{N}_{\rm AF}} \int_0^\beta d\tau \sum_i \vec{S}_i(\tau) e^{i\mathbf{Q}_{\rm AF}\cdot\mathbf{r}_i}, \tag{8}$$

$$\phi^y_{\rm VBS} \equiv \frac{1}{\mathcal{N}_{\rm VBS}} \int_0^\beta d\tau \sum_{\langle i,j\rangle_y} \tau^z_{ij}(\tau) e^{i\mathbf{Q}_{\rm VBS}\cdot\mathbf{r}_{ij}}, \tag{9}$$

where the normalization factors $\mathcal{N}_{\rm AF} = \sqrt{\beta L^2 \chi_{\rm AF}/3}$, $\mathcal{N}_{\rm VBS} = \sqrt{\beta L^2 \chi_{\rm VBS}}$ are defined so that $\langle [\phi^a_{\rm AF}]^2 \rangle = 1$

for $a = 1, 2, 3$ and $\langle [\phi^y_{\rm VBS}]^2 \rangle = 1$. In Fig. 4 (a) we present a histogram of the joint probability distribution of $(\phi^3_{\rm AF}, \phi^y_{\rm VBS})$ at the critical point, h, where the obvious rotational symmetry serves to visualize this emergent symmetry. For comparison, in Fig. 4 (b) we show the analogous histogram at the point of a first order the transition between the same two phase, where only the explicit $Z_2 \times Z_2$ symmetry is present.

It is an established check to examine the $O(4)$ non-invariant moments [11] $F_n \equiv \langle \phi^4 \cos(n\theta) \rangle$ for $n = 2$ and 4 - in polar coordinates, $\phi e^{i\theta} = \phi^3_{\rm AF} + i\phi^y_{\rm VBS}$. Vanishing moments imply an $O(4)$ symmetry. In Table I we observe that at $h = 1.98$ near the critical point h_c, the values for the two moments extrapolate to zero in the thermodynamic and zero temperature limit, strongly indicative of emergent $O(4)$ symmetry.

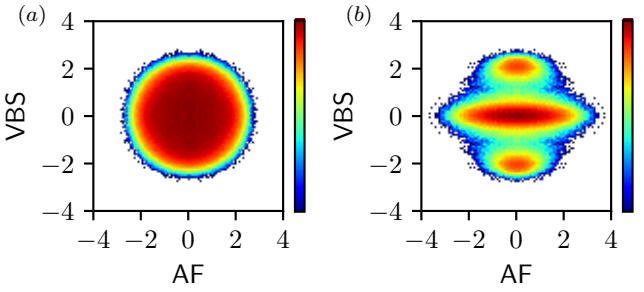

FIG. 4. Histograms for the joint distribution of normalized AF and VBS order parameters $(\phi^3_{\rm AF}, \phi^y_{\rm VBS})$. (a): At a continuous transition between VBS and NAF ($h = 1.98, V = 0.375$ - the filled square in Fig. 1). (b): At a first order transition between VBS and NAF ($h = 1.4, V = 0.40625$ - the empty square in Fig. 1). In both cases, $L = \beta = 16$.

	F_2	F_4
$L = \beta = 10$	0.28 ± 0.04	-0.09 ± 0.03
$L = \beta = 12$	0.20 ± 0.05	-0.08 ± 0.03
$L = \beta = 14$	0.16 ± 0.05	0.06 ± 0.05
$L = \beta = 16$	0.09 ± 0.02	0.05 ± 0.03

TABLE I. Values for $O(4)$ non-invariant moments at $h = 1.98$ - solid square in Fig. 1. Both moments are consistent with zero when extrapolated to the thermodynamic and zero temperature limits.

Topological defects: From the effective field theory perspective, such an unconventional quantum critical point can be described in terms of a non-linear Sigma model (NLSM) with a four-component order parameter (1 for the VBS and 3 for AF orders) augmented by a 2+1 dimensionalθ-topological term [5, 28]. The θ-term connects the AF and VBS orders, so that even away from criticality, one expects the subdominant order parameter to appear where the dominant order is suppressed - especially near topological defects.

At a domain-wall of the VBS order, where $\phi^y_{\rm VBS}$ changes sign (and thus passes through zero) we thus expect that quasi-long range AF order should develop along the VBS domain-wall. In our DQMC study, we can introduce a domain-wall by having an odd number of sites along one of the spatial directions. We examine the real-space version of the AF susceptibility (from Eq. 5)

$$\tilde{\chi}(\mathbf{r}) = \frac{1}{L_x L_y} \sum_i \int_0^\beta d\tau \langle \vec{S}(\mathbf{r}_i, \tau) \cdot \vec{S}(\mathbf{r}_i + \mathbf{r}, 0) \rangle e^{i\mathbf{Q}_{\rm AF}\cdot\mathbf{r}}, \tag{10}$$

where L_x sites is the number of sites in the x-direction and L_y the number of sites in the y-direction. We will consider even values of L_x, and $\mathbf{Q}_{\rm AF} = (\pi, \pi + \delta)$, where δ=0 when L_x is even, and $\delta = -\pi/L_y$ when L_y is odd. When L_y is odd, the VBS order is forced to have a domain wall along the x-direction. We perform such an experiment at $h = 1.1, V = 0.375$, well in the VBS phase. As shown in Fig. 5, when $L_x = 14, L_y = 15$, the long-distance AF correlation is strongly enhanced in the x-direction, along which the domain wall is aligned, while in the $L_x = L_y = 14$ case, the AF correlations are short-ranged [34].

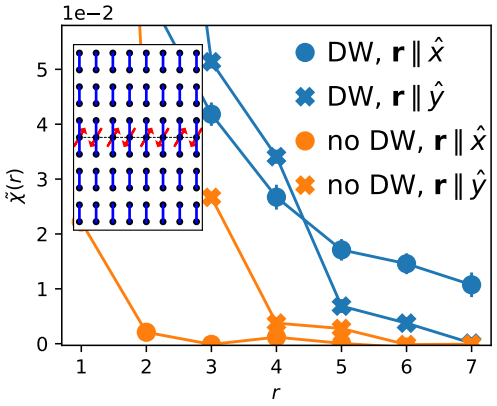

FIG. 5. Real space AF correlations $\tilde{\chi}(\mathbf{r})$ in the VBS phase with ($L_y = 15$) and without ($L_y = 14$) a domain wall (DW) in the VBS order parameter. Here, $h = 1.1, V = 0.375$, $\beta = 16$ and $L_x = 14$, indicated by an empty circle in Fig. 1. The inset is a cartoon of the pseudo-spin configuration with a domain-wall (marked by dashed line), along which AF order is strongly enhanced.

Discussions and Conclusions: Our results demonstrate the occurrence of exotic DQCPs in a model not reverse engineered to produce them. By construction, our system has two extremal (AF and VBS) phases, and by tuning various parameters in the model, it is possible to explore many routes through the phase diagram from one phase to the other. It is notable that we never found a trajectory that gives a direct continuous transition between the two extremal phases, which may be related to the recent findings [29] that the putative DQCP between these two (postulated to have an emergent $SO(5)$

symmetry [28]) may be intrinsically disallowed. On the other hand, the fact that we found that the system found two distinct ways to avoid the $SO(5)$ DQCP is striking - one route being a direct first-order transition between the two phases, and a second route that goes through a DQCP with emergent $SO(4)$ symmetry, via an intermediate NAF phase, and then a second continuous transition. In order to host these two routes, the topology of the phase diagram contains a novel multicritical point, a bicritical point in which one of the phase boundaries is a line of DQCPs.

Some time ago, a nearly continuous transition between VBS and AF phases was observed (using NMR [35]) in $(TMTTF)_2PF_6$, a quasi-2D system with orthorhombic symmetry. Since the C_4 symmetry is already explicitly broken, this transition is equivalent to a VBS to NAF transition. It was speculated that its nearly continuous nature may be related to a lower dimensional (two-dimensional) quantum critical point, which, if true, would be expected on the basis of the present analysis to exhibit an emergent O(4) symmetry.

We acknowledge useful discussions with H. Yao and S. Brown. This work was supported in part by the Department of Energy, Office of Science, Basic Energy Sciences, Material Sciences and Engineering Division, under contract No. DE-AC02-76SF00515 (SAK), and in part by the National Science Foundation (NSF) under Grant No. DMR2000987 (CW and YS). YS was also supported by the Gordon and Betty Moore Foundations EPiQS Initiative through Grants GBMF4302 and GBMF8686, and by the Zuckerman STEM Leadership Program. The numerical simulations were performed on the Sherlock cluster at Stanford University.

[1] R. Blankenbecler, D. J. Scalapino and R. L. Sugar, "Monte Carlo Calculations of Coupled Boson-Fermion Systems," Phys. Rev. D **24**, 2278 (1981).

[2] F. F. Assaad, in "Quantum Simulations of Complex Many- Body Systems: From Theory to Algorithms, Proceedings of Euro Winter School 2002," edited by J. Grotendorst, D. Marx, and A. Muramatsu (John von Neumann Institute for Computing, Jlich, 2002), pp. 99156.

[3] N. Read and S. Sachdev, "Valence-Bond and Spin-Peierls Ground States of Low-Dimensional Quantum Antiferromagnets," Phys. Rev. Lett. **62**, 1694 (1989).

[4] D. S. Rokhsar and S. A. Kivelson, "Superconductivity and the Quantum Hard-Core Dimer Gas," Phys. Rev. Lett. **61**, 2376 (1988).

[5] T. Senthil, L. Balents, S. Sachdev, A. Vishwanath and M. P. A. Fisher, "Quantum Criticality beyond the Landau-Ginzburg-Wilson Paradigm," Phys. Rev. B **70**, 144407 (2004).

[6] A. W. Sandvik, "Evidence for Deconfined Quantum Criticality in a Two-Dimensional Heisenberg Model with Four-Spin Interactions," Phys. Rev. Lett. **98**, 227202 (2007).

[7] R. G. Melko and R. K. Kaul, "Scaling in the Fan of an Unconventional Quantum Critical Point," Phys. Rev. Lett. **100**, 017203 (2008).

[8] J. Lou, A. W. Sandvik and N. Kawashima, "Antiferromagnetic to Valence-Bond-Soild Transitions in Two-Dimensional $SU(N)$ Heisenberg Models with Multi-Spin Interactions," Phys. Rev. B **80**, 180414(R) (2009).

[9] S. Pujari, K. Damle and F. Alet, "Néel-State to Valence-Bond-Solid Transition on the Honeycomb Lattice: Evidence for Deconfined Criticality," Phys. Rev. Lett. **111**, 087203 (2013).

[10] A. Nahum, J. T. Chalker, P. Serna, M. Ortuño and A. M. Somoza, "Deconfined Quantum Criticality, Scaling Violations, and Classical Loop Models," Phys. Rev. X **5**, 041048 (2015).

[11] A. Nahum, P. Serna, J. T. Chalker, M. Ortuño and A. M. Somoza, "Emergent $SO(5)$ Symmetry at the Néel to Valence-Bond-Solid Transition," Phys. Rev. Lett. **115**, 267203 (2015).

[12] T. Okubo, K. Harada, J. Lou and N. Kawashima, "$SU(N)$ Heisenberg Model with Multi-Column Representations," Phys. Rev. B **92**, 134404 (2015).

[13] H. Suwa, A. Sen and A. W. Sandvik, "Level Spectroscopy in a Two-Dimensional Quantum Magnet: Linearly Dispersing Spinons at the Deconfined Quantum Critical Point," Phys. Rev. B **94**, 144416 (2016).

[14] H. Shao, W. Guo and A. W. Sandvik, "Quantum Criticality with Two Length Scales," Science **352**, 213-216 (2016).

[15] Y. Q. Qin, Y.-Y. He, Y.-Z. You, Z.-Y. Lu, A. Sen, A. W. Sandvik, C. Xu and Z. Y. Meng, "Duality between the Deconfined Quantum-Critical Point and the Bosonic Topological Transition," Phys. Rev. X **7**, 031052 (2017).

[16] T. Sato, M. Hohenadler and F. F. Assaad, "Dirac Fermions with Competing Orders: Non-Landau Transition with Emergent Symmetry," Phys. Rev. Lett. **119**, 197203 (2017).

[17] N. Ma, G.-Y. Sun, Y.-Z. You, C. Xu, A. Vishwanath, A. W. Sandvik and Z. Y. Meng, "Dynamical Signature of Fractionalization at a Deconfined Quantum Critical Point," Phys. Rev. B **98**, 174421 (2018).

[18] X.-F. Zhang, Y.-C. He, S. Eggert, R. Moessner and F. Pollmann, "Continuous Easy-Plane Deconfined Phase Transition on the Kagome Lattice," Phys. Rev. Lett. **120**, 115702 (2018).

[19] S. Gazit, F. F. Assaad, S, Sachdev, A. Vishwanath and C. Wang, "Confinement Transition of $\mathbb{Z}_2$ Gauge Theories Coupled to Massless Fermions: Emergent Quantum Chromodynamics and $SO(5)$ Symmetry," Proc. Natl. Acad. Sci. U.S.A **115**, E6987 (2018).

[20] M. Ippoliti, R. S. K. Mong, F. F. Assaad and M. P. Zaletel, "Half-filled Landau levels: A Continuum and Sign-Free Regularization for Three-Dimensional Quantum Critical Points," Phys. Rev. B **98**, 235108 (2018).

[21] G. J. Sreejith, S. Powell and A. Nahum, "Emergent $SO(5)$ Symmetry at the Columnar Ordering Transition in the Classical Cubic Dimer Model," Phys. Rev. Lett. **122**, 080601 (2019).

[22] N. Ma, Y.-Z. You and Z. Y. Meng, "Role of Noethers Theorem at the Deconfined Quantum Critical Point," Phys. Rev. Lett. **122**, 175701 (2019).

[23] Y. Liu, Z. Wang, T. Sato, M. Hohenadler, C. Wang, W. Guo and F. F. Assaad, "Superconductivity from the Condensation of Topological Defects in a Quantum Spin-Hall

Insulator," Nat. Commun. **10**, 2658 (2019).
[24] B. Zhao, P. Weinberg and A. W. Sandvik, "Symmetry Enhanced First-Order Phase Transition in a Two-Dimensional Quantum Magnet," Nat. Phys. **15**, 678 (2019).
[25] P. Serna and A. Nahum, "Emergence and Spontaneous Breaking of Approximate $O(4)$ Symmetry at a Weakly First-Order Deconfined Phase Transition," Phys. Rev. B **99**, 195110 (2019).
[26] Z.-X. Li, S.-K. Jian, and H. Yao, "Deconfined Quantum Criticality and Emergent $SO(5)$ Symmetry in Fermionic Systems," arXiv:1904.10975.
[27] F. Wang, S. A. Kivelson and D.-H. Lee, "Nematicity and Quantum Paramagnetism in FeSe", Nat. Phys. **11**, 959 (2015).
[28] C. Wang, A. Nahum, M. A. Metlitski, C. Xu and T. Senthil, "Deconfined Quantum Critical Points: Symmetries and Dualities," Phys. Rev. X **7**, 031051 (2017).
[29] Y. Nakayama and T. Ohtsuki, "Conformal Bootstrap Dashing Hopes of Emergent Symmetry," Phys. Rev. Lett. **117**, 131601 (2016).
[30] See Supplemental Material [url], which includes Refs. [36-46], for further details.
[31] Our model differs from other, more microscopically simple models, that could in principle describe the same phenomena - for example a Hubbard model with a coupling to both optical and acoustic phonons. However, such models are notoriously difficult to study by any known numerical method, and are analytically tractable only in some version of a weak coupling limit. Here we have designed a model that captures the essence of the same microscopic interactions in the regime where the interplay of the VBS and AF tendencies is prominent. In particular, we represent the lattice distortion by non-electronic pseudo-spins, rather than by a continuous field. We argue that the same physics could be obtained in a model with continuous phonon fields and appropriate phonon-phonon interactions.
[32] As we mention in describing the model, the phonon-phonon interactions naturally lead to nematicity when $V/\tilde{V}$ is sufficiently large and h is sufficiently small. In this limit, the AF order arises due to the electron-electron interactions. Interestingly, the nematic AF order persists beyond this limit as an intermediate phase between AF and VBS phases, and into the vicinity of the AF-NAF-VBS multicritical point.
[33] The small explicit symmetry breaking field shifts the position of the critical points slightly, but does not change their properties.
[34] Direct evidence for the existence of the domain wall for odd L_y can be found in the Supplemental Material [url], which includes Refs. [36-46].
[35] D. S. Chow, P. Wzietek, D. Fogliatti, B. Alavi, D. J. Tantillo, C. A. Merlic and S. E. Brown, "Singular Behavior in the Pressure-Tuned Competition between Spin-Peierls and Antiferromagnetic Ground States of $(TMTTF)_2PF_6$," Phys. Rev. Lett. **81**, 3984 (1998).
[36] J. E. Hirsch, "Discrete Hubbard-Stratonovich Transformation for Fermion Lattice Models," Phys. Rev. B **28**, 4059 (1983).
[37] F. F. Assaad and H. G. Evertz, "World-Line and Determinantal Quantum Monte Carlo Methods for Spins, Phonons and Electrons," in Computational Many-Particle Physics, edited by H. Fehske, R. Schneider and A. Weisse, Springer Berlin Heidelberg **739**, 277 (2008).
[38] Y. Schattner, S. Lederer, S. A. Kivelson, and E. Berg, "Ising Nematic Quantum Critical Point in a Metal: A Monte Carlo Study," Phys. Rev. X **6**, 031028 (2016).
[39] C. Wu and S.-C. Zhang, "Sufficient Condition for Absence of the Sign Problem in the Fermionic Quantum Monte Carlo Algorithm," Phys. Rev. B **71**, 155115 (2005).
[40] F. F. Assaad, "Depleted Kondo Lattices: Quantum Monte Carlo and Mean-Field Calculations," Phys. Rev. B **65**, 115104 (2002).
[41] E. P. Münger and M. A. Novotny, "Reweighting in Monte Carlo and Monte Carlo Renormalization-Group Studies," Phys. Rev. B **43**, 5773 (1991).
[42] K. Binder, "Finite Size Scaling Analysis of Ising Model Block Distribution Functions," Zeitschrift fr Physik B Condensed Matter **43**, 119 (1981).
[43] K. Binder, "Applications of Monte Carlo Methods to Statistical Physics," Rep. Prog. Phys. **60**, 487 (1997).
[44] K. Binder and D. P. Landau, "Finite-Size Scaling at First-Order Phase Transitions," Phys. Rev. B **30**, 1477 (1984).
[45] K. Vollmayr, J. D. Reger, M. Scheucher and K. Binder, "Finite Size Effects at Thermally-Driven First Order Phase Transitions: A Phenomenological Theory of the Order Parameter Distribution," Zeitschrift fr Physik B Condensed Matter **91**, 113 (1993).
[46] S. Iino, S. Morita, A. W. Sandvik and N. Kawashima, "Detecting Signals of Weakly First-Order Phase Transitions in Two-Dimensional Potts Models," J. Phys. Soc. Jpn. **88**, 034006 (2019).